

A Note on the Slim Accretion Disk Model

Wei-Min Gu and Ju-Fu Lu

*Department of Physics and Institute of Theoretical Physics and Astrophysics,
Xiamen University, Xiamen, Fujian 361005, China*

guwm@xmu.edu.cn

ABSTRACT

We show that when the gravitational force is correctly calculated in dealing with the vertical hydrostatic equilibrium of black hole accretion disks, the relationship that is valid for geometrically thin disks, i.e., $c_s/\Omega_K H = \text{constant}$, where c_s is the sound speed, Ω_K is the Keplerian angular velocity, and H is the half-thickness of the disk, does not hold for slim disks. More importantly, by adopting the correct vertical gravitational force in studies of thermal equilibrium solutions, we find that there exists a maximally possible accretion rate for each radius in the outer region of optically thick accretion flows, so that only the inner region of these flows can possibly take the form of slim disks, and strong outflows from the outer region are required to reduce the accretion rate in order for slim disks to be realized.

Subject headings: accretion, accretion disks — black hole physics — hydrodynamics

1. Introduction

The slim disk model is one of popular models for accretion flows around black holes and has been applied in recent years to quite many energetic astrophysical systems such as narrow line Seyfert 1 galaxies (e.g., Wang & Netzer 2003; Chen & Wang 2004), Galactic black hole candidates (e.g., Watarai et al. 2000), and ultraluminous X-ray sources (e.g., Watarai, Mizuno, & Mineshige 2001; Vierdaynti et al. 2006).

Despite of its growing importance in the observational sense, we notice that some theoretical problems regarding to this model in the fundamental sense have been ignored. In this paper we address one such problem, namely the inaccurate calculation of the gravitational force in dealing with the hydrostatic equilibrium in the vertical direction of slim disks. We work in the cylindrical coordinate system (r, z, φ) throughout.

2. Vertical gravitational force

Obviously because the Shakura-Sunyaev disk (SSD) model (Shakura & Sunyaev 1973) is the first and still the most successful model of accretion disks, many simplifications made in this model are followed by the subsequent accretion disk models without rigorously verifying their applicability. The treatment of the disk’s vertical structure is such a one.

The very basic character of an SSD is that it is geometrically thin, i.e., everywhere in the disk the half thickness $H(r)$ is much smaller than the corresponding cylindrical radius r , $H(r)/r \ll 1$. This means that the averaged motion of disk matter in the vertical direction (if there is any) must be negligible comparing with that in the radial direction, and it is reasonable to assume that in the macro sense the disk matter is in the vertical hydrostatic equilibrium, i.e., in the vertical direction the gravitational force and the pressure force are balanced with each other,

$$\frac{\partial p}{\partial z} + \rho \frac{\partial \psi}{\partial z} = 0, \quad (1)$$

where p is the pressure, ρ is the mass density, ψ is the gravitational potential, and the disk is already assumed to be steady and axisymmetric, $\partial/\partial t = \partial/\partial \varphi = 0$. In the SSD model the Newtonian potential $\psi_N(r, z) = -GM/\sqrt{r^2 + z^2}$ was used, where M is the mass of central accreting object, and the one-zone approximation in the vertical direction was made; then in equation (1) $\partial p/\partial z \simeq -p/H$, $\partial \psi_N/\partial z \simeq GMH/r^3 = \Omega_K^2 H$, where $\Omega_K = (GM/r^3)^{1/2}$ is the Keplerian angular velocity, and a relation $H = c_s/\Omega_K$ was obtained, where $c_s = (p/\rho)^{1/2}$ is the sound speed (e.g., Kato, Fukue, & Mineshige 1998, p. 80).

The above procedure was somewhat improved by Hōshi (1977), who approximated the Newtonian potential as $\psi_N(r, z) \simeq \psi_N(r, 0) + \Omega_K^2 z^2/2$ and assumed a polytropic relation in the vertical direction, $p = K\rho^{1+1/N}$, where K and N are constants, instead of the one-zone approximation. Then the disk becomes to have a vertical structure, and the vertical integration of equation (1) gives $H = \sqrt{2(N+1)}c_s/\Omega_K$, where the sound speed $c_s = (p_0/\rho_0)^{1/2}$, with subscript 0 representing quantities on the equatorial plane.

Both the SSD model and Hōshi (1977) reduced the differential equation (1) into a very simple but very useful relation: $c_s/\Omega_K H = \text{constant}$. This relation was adopted in the slim disk model in the following way. First, the vertical hydrostatic equilibrium was still assumed, even though slim disks are not geometrically thin, i.e., they may have $H \lesssim r$ or $H \sim r$. The argument for this was that these disks have quite large radial velocities, so that their configurations are quasi-spherical, i.e., the vertical motion of disk matter can still be safely neglected, and equation (1) holds. Second, although the pseudo-Newtonian potential

introduced by Paczyński & Wiita (1980, hereafter the PW potential), i.e.,

$$\psi_{\text{PW}}(r, z) = -GM_{\text{BH}}/(\sqrt{r^2 + z^2} - r_{\text{g}}), \quad (2)$$

was widely used to simulate the general relativistic effect of central black hole, where M_{BH} is the black hole mass and $r_{\text{g}} \equiv 2GM_{\text{BH}}/c^2$ is the Schwarzschild radius, it was again treated in the form of Hōshi (1977), i.e.,

$$\psi_{\text{PW}}(r, z) \simeq \psi_{\text{PW}}(r, 0) + \Omega_{\text{K}}^2 z^2 / 2, \quad (3)$$

where the Keplerian angular velocity $\Omega_{\text{K}} = (GM/r)^{1/2}/(r - r_{\text{g}})$. Using equation (3) and keeping the assumption of polytropic relation, the relation $c_{\text{s}}/\Omega_{\text{K}}H = \text{constant}$ was refined by integrating equation (1), with the sound speed c_{s} being defined either in terms of the pressure and mass density on the equatorial plane (Abramowicz et al. 1988; Wang & Zhou 1999; Chen & Wang 2004), or in terms of the vertically integrated pressure and density, i.e., $c_{\text{s}} = (\Pi/\Sigma)^{1/2}$, where $\Pi = \int_{-H}^H p dz$ and $\Sigma = \int_{-H}^H \rho dz$ (Kato et al. 1998, p. 242; Watarai 2006).

To check the validity of the Hōshi form of potential, we draw in Figure 1 the gravitational force in the vertical direction $\partial\psi_{\text{PW}}/\partial z$ in units of (c^2/r_{g}) for varying values of (z/r) at a fixed radius $r = 10r_{\text{g}}$, calculated from equations (2) (the solid line) and (3) (the dashed line), respectively. It is as expected that the Hōshi form of potential equation (3) is valid only for $(z/r) \lesssim 0.2$, while for $(z/r) \sim 1$ it greatly magnifies the vertical gravitational force comparing with the correct result according to the explicit form of the PW potential equation (2).

In the following calculations we take the polytropic index $N = 3$. Instead of the simple relationships $(\rho/\rho_0)^{1/3} = (p/p_0)^{1/4} = 1 - (z/H)^2$ and $8p_0/\rho_0 = \Omega_{\text{K}}^2 H^2$ obtained using equation (3) (Kato et al. 1998, p. 241), the vertical integration of equation (1) using equation (2) gives

$$\left(\frac{\rho}{\rho_0}\right)^{1/3} = \left(\frac{p}{p_0}\right)^{1/4} = \frac{\frac{1}{\sqrt{1+(z/r)^2-r_{\text{g}}/r}} - \frac{1}{\sqrt{1+(H/r)^2-r_{\text{g}}/r}}}{\frac{1}{1-r_{\text{g}}/r} - \frac{1}{\sqrt{1+(H/r)^2-r_{\text{g}}/r}}}, \quad (4)$$

$$4\frac{p_0}{\rho_0} = \Omega_{\text{K}}^2 r^2 (1 - r_{\text{g}}/r) \left[1 - \frac{1 - r_{\text{g}}/r}{\sqrt{1 + (H/r)^2 - r_{\text{g}}/r}} \right]. \quad (5)$$

For a fixed r and a given value of H/r , we obtain values of $(\Sigma/2\rho_0 H)$ and $(\Pi/2p_0 H)$ by vertically integrating equation (4), and value of $(c_{\text{s}}/\Omega_{\text{K}}H)$ by using equation (5). We define $c_{\text{s}}^2 = \Pi/\Sigma$ as in Kato et al. (1998), where detailed results were provided and can be quantitatively compared with ours.

Figure 2 shows $\Sigma/2\rho_0H$ (the dashed line), $\Pi/2p_0H$ (the dotted line), and c_s/Ω_KH (the solid line) as functions of H/r at $r = 10r_g$. In the slim disk model these three quantities were all constant, for $N = 3$ they were: $\Sigma/2\rho_0H = 16/35$, $\Pi/2p_0H = 128/315$, and $c_s/\Omega_KH = 1/3$ (Kato et al. 1998, p. 242). It is seen from the figure that, however, these quantities are not constant, they take approximately their model-predicted values only for $H/r \ll 1$. For slim disks with $H/r \sim 1$, the simple relation $c_s/\Omega_KH = \text{constant}$ is invalid.

3. Thermal equilibria

To reveal further the consequence of the correction of vertical gravitational force, we go on to study thermal equilibrium solutions of black hole accretion flows. We write the continuity, radial momentum, angular momentum, energy, and state equations of accretion flows in the form similar to that of Kato et al. (1998):

$$\dot{M} = -2\pi r \Sigma v_r = \text{const.} , \quad (6)$$

$$v_r \frac{dv_r}{d \ln r} + c_s^2 \frac{d \ln \Pi}{d \ln r} - \Omega^2 r^2 = -\frac{\Omega_K^2 (r - r_g)^2}{\Sigma} \int_{-H}^H \frac{\rho}{[\sqrt{1 + (z/r)^2} - r_g/r]^2 \sqrt{1 + (z/r)^2}} dz , \quad (7)$$

$$\dot{M}(\Omega r^2 - j_0) = 2\pi \alpha r^2 \Pi , \quad (8)$$

$$Q_{\text{vis}}^+ = Q_{\text{adv}}^- + Q_{\text{rad}}^- , \quad (9)$$

$$\Pi = \Pi_{\text{gas}} + \Pi_{\text{rad}} = \frac{k_B \rho_0 T_0}{\mu m_p} \int_{-H}^H \left(\frac{\rho}{\rho_0} \right) \left(\frac{T}{T_0} \right) dz + \frac{1}{3} a T_0^4 \int_{-H}^H \left(\frac{T}{T_0} \right)^4 dz , \quad (10)$$

where \dot{M} is the mass accretion rate, v_r is the radial velocity, Ω is the angular velocity, j_0 is an integration constant representing the specific angular momentum (per unit mass) accreted by the black hole, and α is the viscosity parameter. Equation (7) is obtained by vertically integrating equation (8.2) of Kato et al. (1998) and specifying the PW potential equation (2). The viscous heating rate is $Q_{\text{vis}}^+ = \dot{M} \Omega^2 f g / 2\pi$, where $f = 1 - j/\Omega_K r^2$, $j = j_0/\omega$, $\omega = \Omega/\Omega_K$ is assumed to be a constant that is smaller than 1 (sub-Keplerian rotation) and is to be evaluated, and $g = -d \ln \Omega_K / d \ln r$. The advective cooling rate is $Q_{\text{adv}}^- = \xi \dot{M} c_s^2 / 2\pi r^2$ (see Kato et al. 1998 for the detailed expression of ξ). The radiative cooling rate is $Q_{\text{rad}}^- = 32\sigma T_0^4 / 3\tau$, where T_0 is the temperature on the equatorial plane, $\tau = \kappa_{\text{es}} \rho_0 H$ is the vertical optical depth (e.g., Eq. [8.61] of Kato et al. 1998), and $\kappa_{\text{es}} \simeq 0.34 \text{ cm}^2 \text{ g}^{-1}$ is the electron scattering opacity

that is assumed to be the dominant opacity source. In equation (10) T is the temperature, and $T/T_0 = (\rho/\rho_0)^{1/3}$ as expressed by equation (4). For slim disks the radiation pressure dominates over the gas pressure, so the term Π_{gas} in equation (10) can be dropped for the moment.

To avoid unnecessary complicacy, we ignore the ram pressure term $v_r dv_r / \ln r$ in equation (7), and take $\ln \Pi / \ln r = -3/2$ and $\xi = 3/2$ from the self-similar solution (e.g., Wang & Zhou 1999; Watarai 2006). Then we have a set of six algebraic equations, i.e., equations (5-10), which can be solved for six unknown quantities H , v_r , c_s , Ω (or ω), ρ_0 , and T_0 , with given values of M_{BH} , \dot{M} , α , j , and r . In our calculations we fix $M_{\text{BH}} = 10M_{\odot}$, $\alpha = 0.1$, and $j = 1.83cr_g$ (a reasonable value that is just a little less than the Keplerian angular momentum at the last stable orbit, $\Omega_K r^2|_{3r_g} = 1.837cr_g$).

Figure 3 shows thermal equilibrium solutions at a certain radius in the form of $\dot{m} - H/r$ plane, where \dot{m} is the accretion rate normalized by the Eddington accretion rate $\dot{M}_{\text{Edd}} = 64\pi GM_{\text{BH}}/c\kappa_{\text{es}}$. The thick lines represent the solutions obtained with the PW potential equation (2). For comparison, the thin lines draw the solutions obtained with the Hōshi form of potential equation (3), and accordingly equation (7) is reduced to equation (2.9) of Matsumoto et al. (1984). The dashed, solid, and dotted lines are for $r = 5r_g$, $r = 50r_g$, and $r = 500r_g$, respectively. It is seen that for $r = 5r_g$, the difference between the results obtained with two potentials is only quantitative. For $r = 50r_g$ and $r = 500r_g$, however, the difference becomes qualitative. The most remarkable is that the thick solid and thick dotted lines have a maximum (not drawn in the figure), i.e., there exists a maximally possible accretion rate \dot{m}_{max} for slim disk solutions in the PW potential, while no such a \dot{m}_{max} exists for solutions in the Hōshi form of this potential (the thin solid and thin dotted lines). One might wonder whether $H/r > 1$, at which \dot{m}_{max} appears, is physical. Our arguments are the following. First, $H/r > 1$ has indeed been obtained in many works on slim disks or other accretion disks (see, e.g., Figs. 5-10 of Peitz & Appl 1997; Figs. 1-4 of Popham & Gammie 1998; Figs. 4 and 6 of Lu, Gu, & Yuan 1999; Fig. 5 of Chen & Wang 2004; Figs. 3 and 5 of Watarai 2006). Second, it does not matter for which value of H/r this \dot{m}_{max} really appears. What is important is that for each large radius there is an upper limit for \dot{m} , beyond which no thermal equilibrium solutions can be constructed. By contrast, the previous understanding in the slim disk model (e.g., Abramowicz et al. 1988; Chen et al. 1995; Kato et al. 1998) was that any large \dot{m} can correspond to a thermal equilibrium solution, as the thin solid and thin dotted lines in Figure 3 imply. This is because those authors either used the Hōshi form of potential equation (3) that magnifies the vertical gravitational force, or used the relation $c_s/\Omega_K H = \text{constant}$ that is resulted from equation (3).

It is also noticeable that at small radii ($r = 5r_g$ in Fig. 3) there is no \dot{m}_{max} for thermal

equilibrium solutions. Figure 4 illustrates this qualitative difference between small and large radii. Figure 4(a) is for $\dot{m} = 10$ and $r = 5r_g$, Figure 4(b) is also for $\dot{m} = 10$ but for $r = 50r_g$ (\dot{m} is larger than the corresponding \dot{m}_{\max}). It is clear that in the former case the thermal equilibrium can be established, i.e., $Q_{\text{vis}}^+ = Q^-$ ($\equiv Q_{\text{adv}}^- + Q_{\text{rad}}^-$), or $Q_{\text{vis}}^+ = Q_{\text{adv}}^-$ if Q_{rad}^- is totally negligible, can be realized for some value of $H/r \sim 1$; while in the latter case there are no thermal equilibrium solutions as Q_{vis}^+ is always larger than Q^- .

We derive an approximate analytic expression of the critical radius r_{crit} , for $r > r_{\text{crit}}$ there is a \dot{m}_{\max} and for $r < r_{\text{crit}}$ there is not. Equation (5) gives $4c_s^2 < \Omega_K^2 r^2$, and equation (7) gives $(3/2)c_s^2 + \Omega^2 r^2 \simeq \Omega_K^2 r^2$, so we have $(5/2)c_s^2 < \Omega^2 r^2$. As seen from Figure 4, the condition that can ensure a thermal equilibrium solution at a radius is $Q_{\text{adv}}^- \geq Q_{\text{vis}}^+$, i.e., $(3/2)c_s^2/r^2 \geq \Omega^2 f g \simeq (3/2)\Omega^2 f$ since $g \simeq 3/2$. Therefore, the criterion for a thermal equilibrium solution to exist is expressed as

$$f \equiv 1 - \frac{j}{\Omega_K r^2} \leq \frac{2}{5}. \quad (11)$$

For $j = 1.83cr_g$ in our calculations, the critical value $f_{\text{crit}} = 2/5$ gives $r_{\text{crit}} = 16.4r_g$, which agrees well with the numerical value $r_{\text{crit}} = 18.8r_g$ in Figures 3 and 5. The reason why f is of crucial importance is that since Q_{vis}^+ is proportional to f , for small radii f is small, and Q_{vis}^+ can be balanced by Q_{adv}^- for any \dot{m} ; while for large radii f is large, there must be an upper limit for \dot{m} , beyond which Q_{vis}^+ would be too large to be balanced by any cooling.

To see where the position of slim disks is according to our understandings, we present in Figure 5 a united description of thermal equilibrium solutions of optically thick accretion flows around black holes in the form of $\dot{m}-r$ plane. The solid line in the figure draws \dot{m}_{\max} for each radius, above which no thermal equilibrium solutions exist at all. The rest of the plane is further divided into three regions based on the local stability analysis. We adopt a simple thermal instability criterion: $(\partial Q_{\text{vis}}^+/\partial T)_{\Sigma} - (\partial Q^-/\partial T)_{\Sigma} > 0$, which is practically valid for moderately large-scale perturbations (Kato et al. 1998, p. 306). The criterion results in: $\delta = 2 - 5\beta - 6f_{\text{adv}} + 8\beta f_{\text{adv}} > 0$, where $\beta \equiv \Pi_{\text{gas}}/\Pi$, and $f_{\text{adv}} \equiv Q_{\text{adv}}^-/Q_{\text{vis}}^+$. The dotted and dashed lines both draw $\delta = 0$, but correspond to $\beta = 2/5$ and $f_{\text{adv}} = 0$, and to $f_{\text{adv}} = 1/3$ and $\beta = 0$, respectively. The region below the dotted line has $\delta < 0$ and is for stable SSDs, which are radiative cooling-dominated ($f_{\text{adv}} \rightarrow 0$) and gas pressure-supported ($\beta > 2/5$). The region between the dotted and the dashed lines has $\delta > 0$ and is for unstable SSDs, which are radiation pressure-supported ($\beta < 2/5$) but not yet advective cooling-dominated ($f_{\text{adv}} < 1/3$). These two regions were already known in the literature. The region between the dashed and the solid line has $\delta < 0$ and is obviously for slim disks, which are advective cooling-dominated ($f_{\text{adv}} > 1/3$) and radiation pressure-supported ($\beta \rightarrow 0$), and are stable. What is new is that, because of the limitation of \dot{m}_{\max} , accretion flows can possibly take the form of slim disks only in the inner region, i.e., in the region $r < r_{\text{crit}}$.

Figure 5 may have interesting implications. If the accretion rate \dot{m} of an accretion flow is sufficiently small at large radii (i.e., below the dotted line), then the flow can behave as an SSD throughout (here we don't want to discuss the inability of SSD model for the inner region of a black hole accretion flow, such as for the flow's transonic motion). If, however, \dot{m} at large radii is in the unstable region or in the no-solution region, then it seems that the only possible way for accretion to proceed is that the flow loses its matter continuously in the form of outflows. Such outflows must be so strong that \dot{m} keeps being below the dotted line all the way till the inner region $r < r_{\text{crit}}$. In the inner region there are two possibilities for the accretion flow: either \dot{m} is still below the dotted line and the flow keeps being an SSD, or \dot{m} is in the unstable region. In the latter case the flow may undergo a limit cycle, i.e., oscillating between the SSD state and the slim disk state in the vertical axis direction of Figure 5. Such a limit cycle behavior has been investigated extensively in the literature (e.g., Szuszkiewicz & Miller 2001 and references therein), and is the likely way for slim disks to be realized. A related remark is that provided \dot{m} in the outer region of accretion flows is not sufficiently small, outflows seem to be unavoidable, as already observed in many high energy astrophysical systems that are believed to be powered by black hole accretion.

4. Discussion

We have shown that when the gravitational force in the vertical direction of black hole accretion disks is correctly calculated, the relationship $c_s/\Omega_K H = \text{constant}$, which is valid only for geometrically thin disks, does not hold for slim disks; and that there exists a maximally possible mass accretion rate for each radius in the outer region of optically thick accretion flows, so that only the flow's inner region can possibly take the form of slim disks, and outflows from the outer region must be produced in order for slim disks to be realized. We stress that only one change has been made in obtaining these results, i.e., using the explicit form of the PW potential, instead of the Hōshi form of this potential, to calculate the vertical gravitational force, while all the assumptions, equations, and methods for solutions are kept exactly the same as in the slim disk model (e.g., in the excellent book of Kato et al. 1998).

All our results here are based on a local analysis. Though the similar local analysis was often used in the literature (e.g., Abramowicz et al. 1995; Chen et al. 1995; Kato et al. 1998), it is worth checking our results by constructing global solutions of original differential equations for black hole accretion flows, like what was done by, e.g., Chen & Wang (2004), but with a revised vertical gravitational force. We plan to do this in a subsequent work.

A natural question is why we concentrate our attention here only on slim disks and

do not touch another type of black hole accretion flows, namely optically thin advection-dominated accretion flows (ADAFs, Narayan & Yi 1994; Abramowicz et al. 1995), which are also geometrically not thin. We think that the ADAF model is also likely to suffer the same problem in the vertical direction as the slim disk model does, because the problem is resulted from a purely hydrodynamic consideration and is related only to the geometrical thickness of the flow. In particular, the usage of relation $c_s/\Omega_K H = \text{constant}$ for ADAFs is questionable. What is different is that for optically thin flows the radiation processes are more complicated and the vertical integration is not as easy to perform as for slim disks. In addition, ADAFs are known to correspond to very low accretion rates and to have a maximally possible accretion rate at each radius (e.g., Abramowicz et al. 1995), so the problem may have no impact on ADAFs in respect of the accretion rate. However, we still wish to make one more comment. Many 2-dimensional or 3-dimensional numerical simulations of viscous radiatively inefficient accretion flows revealed the existence of convection-dominated accretion flows instead of ADAFs (e.g., Stone, Pringle, & Begelman 1999; Igumenshchev & Abramowicz 2000; McKinney & Gammie 2002; Igumenshchev, Narayan, & Abramowicz 2003). According to our results here, the 1-dimensional ADAF model might have hidden inconsistencies in the vertical direction, so that ADAFs could not be obtained in those multidimensional numerical simulations.

We thank Li Xue for beneficial discussion and the referee for prompt and helpful comments. This work was supported by the National Science Foundation of China under Grants No. 10503003 and 10673009.

REFERENCES

- Abramowicz, M. A., Chen, X., Kato, S., Lasota, J.-P., & Regev, O. 1995, *ApJ*, 438, L37
- Abramowicz, M. A., Czerny, B., Lasota, J.-P., & Szuszkiewicz, E. 1988, *ApJ*, 332, 646
- Chen, L.-H., & Wang, J.-M. 2004, *ApJ*, 614, 101
- Chen, X., Abramowicz, M. A., Lasota, J.-P., Narayan, R., & Yi, I. 1995, *ApJ*, 443, L61
- Hōshi, R. 1977, *Prog. Theor. Phys.*, 58, 1191
- Igumenshchev, I. V., & Abramowicz, M. A. 2000, *ApJS*, 130, 463
- Igumenshchev, I. V., Narayan, R., & Abramowicz, M. A. 2003, *ApJ*, 592, 1042

- Kato, S., Fukue, J., & Mineshige, S. 1998, *Black-Hole Accretion Disks* (Kyoto: Kyoto Univ. Press)
- Lu, J.-F., Gu, W.-M., & Yuan, F. 1999, *ApJ*, 523, 340
- Matsumoto, R., Kato, S., Fukue, J., & Okazaki, A. 1984, *PASJ*, 36, 71
- McKinney, J. C., & Gammie, C. F. 2002, *ApJ*, 573, 728
- Narayan, R., & Yi, I. 1994, *ApJ*, 428, L13
- Paczyński, B., & Wiita, P. J. 1980, *A&A*, 88, 23
- Peitz, J., & Appl, S. 1997, *MNRAS*, 286, 681
- Popham, R., & Gammie, C. F. 1998, *ApJ*, 504, 419
- Shakura, N. I., & Sunyaev, R. A. 1973, *A&A*, 24, 337
- Stone, J. M., Pringle, J. E., & Begelman, M. C. 1999, *MNRAS*, 310, 1002
- Szuskiewicz, E., & Miller, J. C. 2001, *MNRAS*, 328, 36
- Vierdayanti, K., Mineshige, S., Ebisawa, K., & Kawaguchi, T. 2006, *PASJ*, 58, 915
- Wang, J.-M., & Netzer, H. 2003, *A&A*, 398, 927
- Wang, J.-M., & Zhou, Y.-Y. 1999, *ApJ*, 516, 420
- Watarai, K. 2006, *ApJ*, 648, 523
- Watarai, K., Fukue, J., Takeuchi, M., & Mineshige, S. 2000, *PASJ*, 52, 133
- Watarai, K., Mizuno, T., & Mineshige, S. 2001, *ApJ*, 549, L77

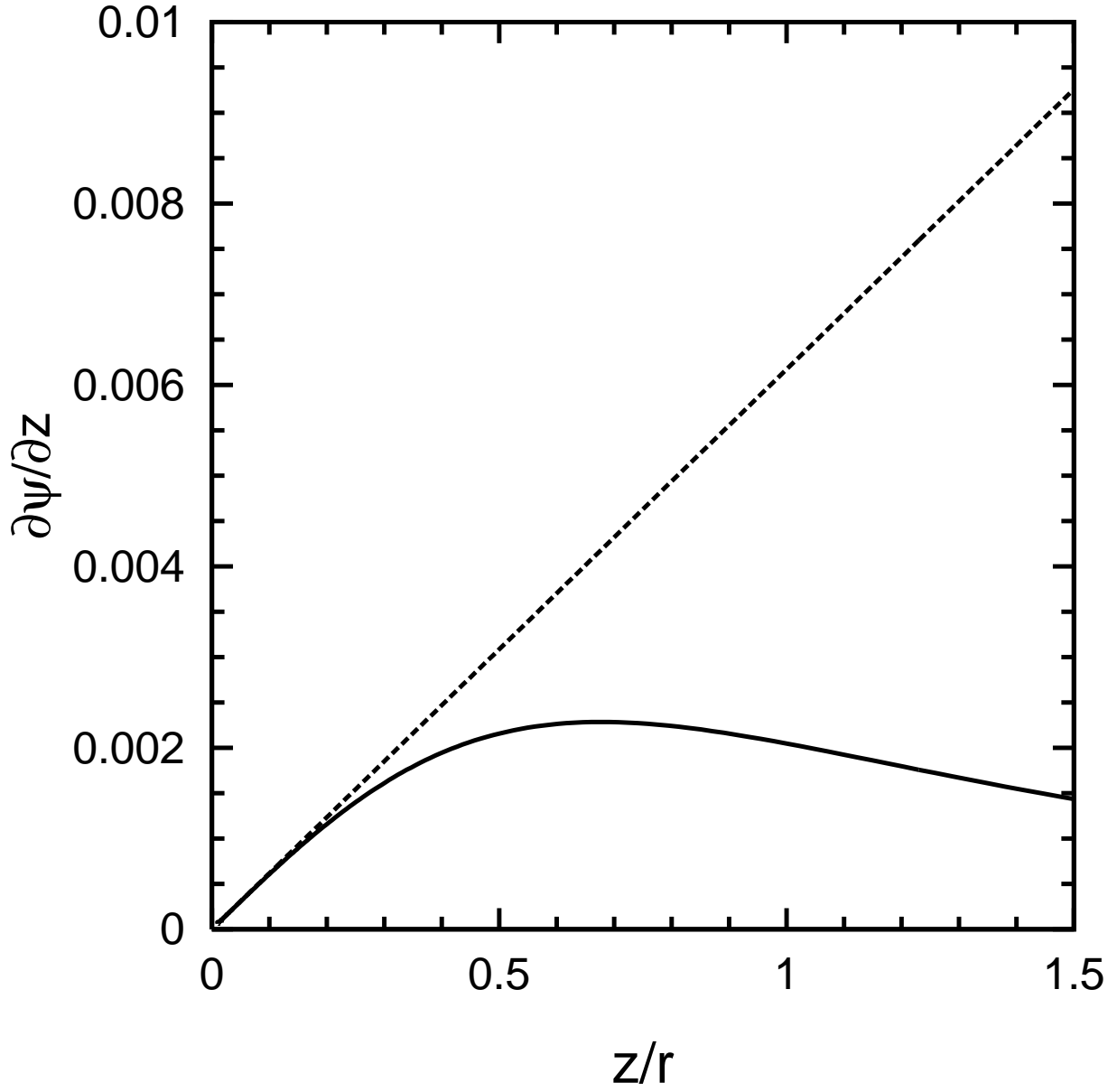


Fig. 1.— Vertical gravitational force $\partial\psi/\partial z$ for varying z/r at $r = 10r_g$, calculated using the explicit form of the PW potential (the solid line) and the Hōshi form of this potential (the dashed line), respectively.

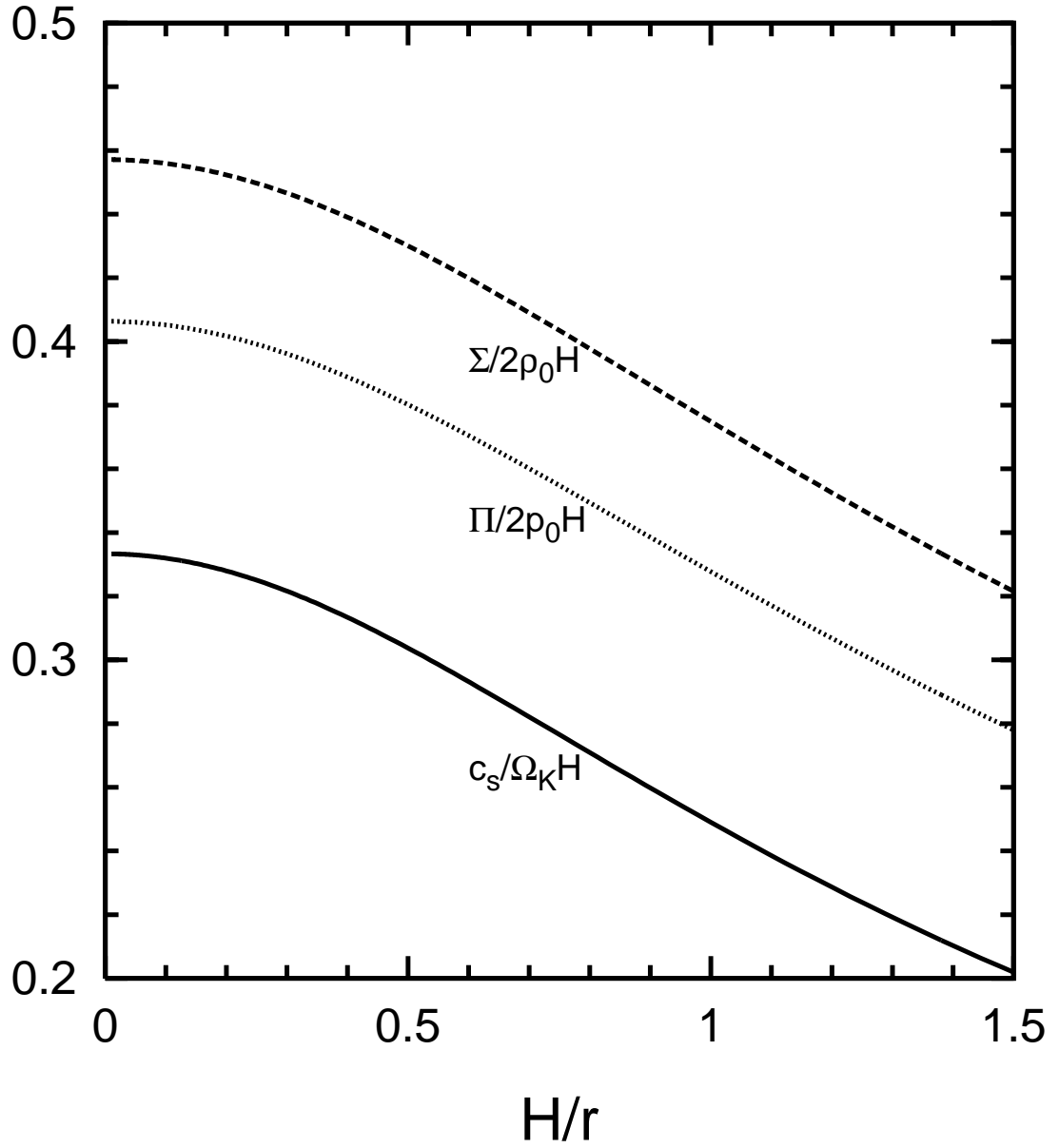


Fig. 2.— Variations of $\Sigma/2\rho_0 H$ (the dashed line), $\Pi/2p_0 H$ (the dotted line), and $c_s/\Omega_K H$ (the solid line) with H/r at $r = 10r_g$.

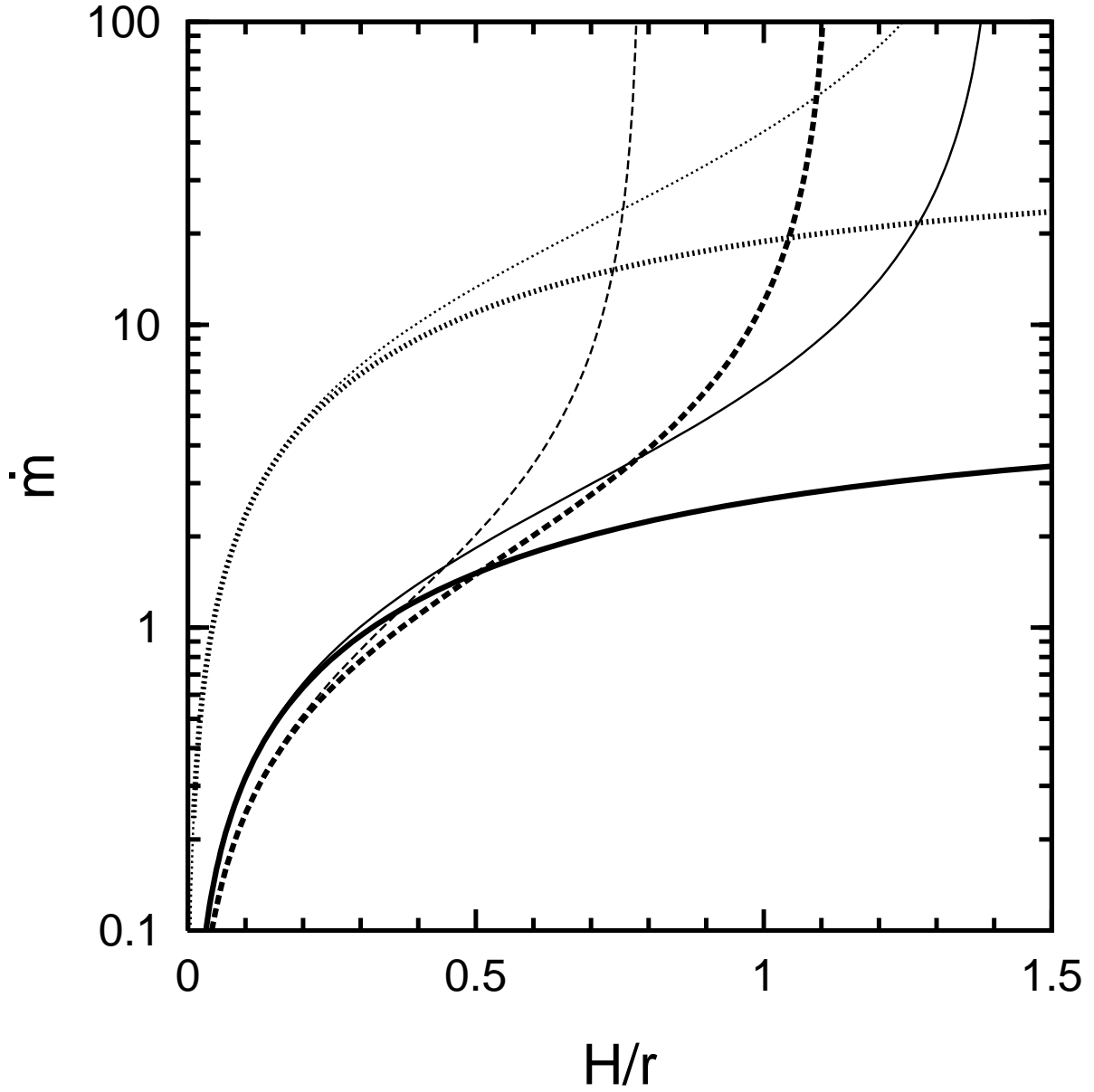


Fig. 3.— Thermal equilibrium solutions with the Hōshi form of the PW potential (thin lines) and with the explicit PW potential (thick lines) at $r = 5r_g$ (dashed lines), $r = 50r_g$ (solid lines), and $r = 500r_g$ (dotted lines).

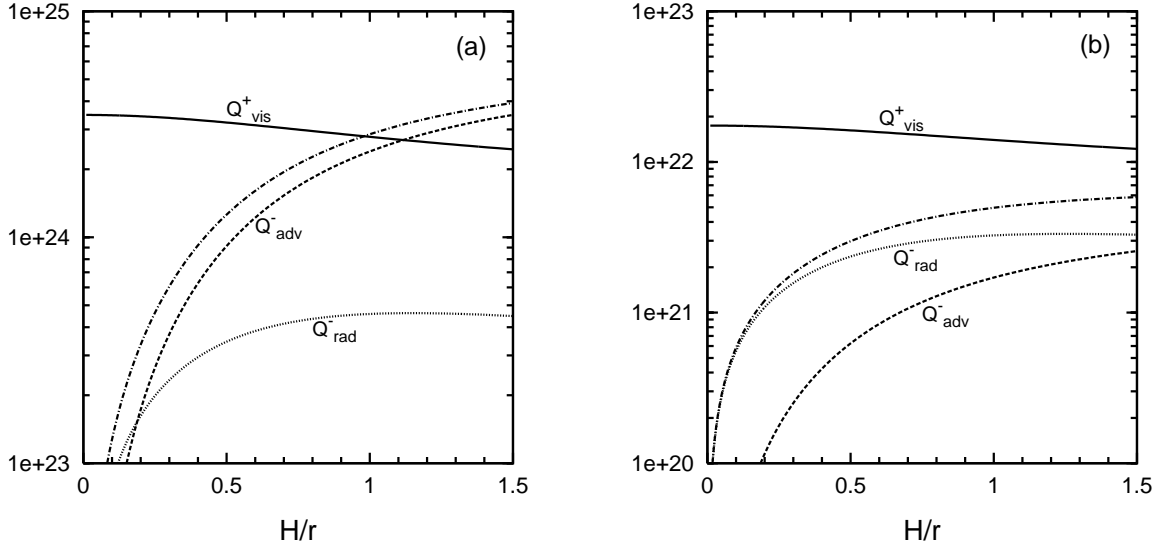


Fig. 4.— Variations of Q_{vis}^+ (the solid line), Q_{adv}^- (the dashed line), Q_{rad}^- (the dotted line), and $Q_{\text{adv}}^- + Q_{\text{rad}}^-$ (the dot-dashed line) with H/r . (a) is for $\dot{m} = 10$ and $r = 5r_g$, (b) is for $\dot{m} = 10$ and $r = 50r_g$. Numbers attaching the vertical axis are in units of $\text{erg cm}^{-2}\text{s}^{-1}$.

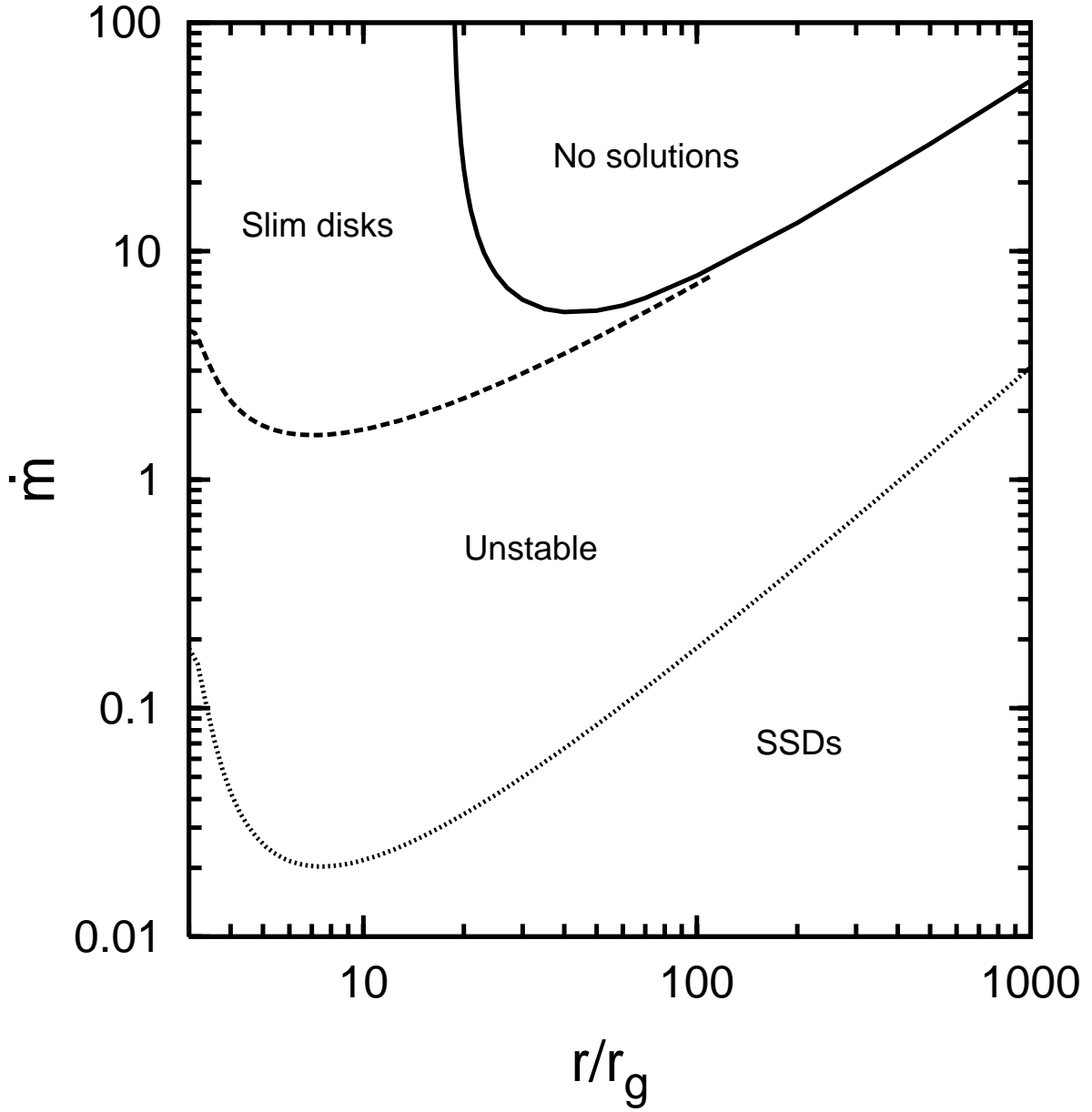


Fig. 5.— Distribution of thermal equilibrium solutions. The solid line is for m_{\max} , the dashed line for $f_{\text{adv}} = 1/3$, and the dotted line for $\beta = 2/5$.